Structure of the Tet Repressor–Tetracycline Complex and Regulation of Antibiotic Resistance

Winfried Hinrichs,* Caroline Kisker, Martina Düvel, Alexander Müller, Karlheinz Tovar, Wolfgang Hillen, Wolfram Saenger*

The most frequently occurring resistance of Gram-negative bacteria against tetracyclines is triggered by drug recognition of the Tet repressor. This causes dissociation of the repressor-operator DNA complex and enables expression of the resistance protein TetA, which is responsible for active efflux of tetracycline. The 2.5 angstrom resolution crystal structure of the homodimeric Tet repressor complexed with tetracycline-magnesium reveals detailed drug recognition. The orientation of the operator-binding helix-turn-helix motifs of the repressor is inverted in comparison with other DNA binding proteins. The repressor-drug complex is unable to interact with DNA because the separation of the DNA binding motifs is 5 angstroms wider than usually observed.

The emergence and rapid distribution in recent years of different resistance mechanisms of bacteria against antibiotics has severely reduced our ability to combat infectious diseases (*1*). Tetracyclines (Tcs) are among the most commonly used broad spectrum antibiotics (*2*). Their antibiotic action interrupts polypeptide chain elongation.

The most abundant resistance mechanism against Tcs in Gram-negative bacteria is based on active export of the drug. The resistance protein TetA couples the efflux of Tc in complex with a divalent metal ion (Mg^{2+}) to the uptake of a proton (*3*). Tet repressor (TetR) regulates the expression of this antiporter at the level of transcription and is induced by a $[Mg\text{-}Tc]^+$ complex. In the absence of Tc, TetR binds to two tandem operators of nearly identical palindromic sequences, thereby preventing expression of TetR and TetA (*4*). Because the affinity of $[Mg\text{-}Tc]^+$ for TetR (association constant $K_a \sim 10^9\ M^{-1}$) is much stronger than for the ribosome ($K_a \sim 10^6\ M^{-1}$), the expression of the resistance protein is initiated, and Tc is removed from the cell before inhibition of protein biosynthesis occurs (*5*).

The crystal structure of the class D TetR ($TetR^D$) (*6*) in complex with $[Mg\text{-}Tc]^+$ was determined at 2.5 Å resolution (Table 1). The asymmetric unit of the crystal unit cell contains the $TetR^D$ monomer with one Tc and one Mg^{2+} bound. The polypeptide folds into 10 α helices, α1 to α10, with connecting turns and loops (Fig. 1A). Two monomers are related by a crystallographic twofold axis to form a dimer, which is clearly divided into the protein core and the two DNA binding domains.

The core, helices α5 to α10, is responsible for dimer stability. It is the regulatory domain of $TetR^D$ because it harbors the Tc binding pocket, which is composed of the COOH-termini of α4 and α6 and the helices α5, α7, α8, α8′, and α9′ (a prime refers to the second unit of the dimer) (Fig. 1A). The dimerization of $TetR^D$ occurs through a surface formed by helices α7 to α10 and the interconnecting loops. The antiparallel helices α8 and α10 intersect with the symmetry-related α8′ and α10′ at an angle of ~80° to establish a four-helix bundle around the twofold axis. Additional interactions of the two monomers occur between α9 and α7′ and the loop connecting α8 and α9, which is in contact with the loop connecting α6′ and α7′.

The DNA binding domains in the $TetR^D$ dimer are represented by the symmetry-related three-helix bundles α1 to α3 and α1′ to α3′ and connected to the protein core by α4 and α4′, respectively. They include the helix-turn-helix (HTH) motif (α2-turn-α3) and are stabilized by hydrophobic interactions, in agreement with biochemical data (*7*). The HTH motifs are isostructural to the HTH motifs in factor of inversion stimulation (FIS), catabolite activator protein, and the repressors cro, λcI, 434, and *trp* (*8*), with root-mean-square (rms) deviations ranging from 0.5 to 0.8 Å if Cα positions are superimposed. However, the recognition helix α3 in $TetR^D$ is about one turn shorter at the COOH-terminus than those in other HTH motifs (*9*) or as proposed (*10*) for TetR.

The orientation of the two HTH motifs is inverted with respect to all presently known crystal structures of proteins containing this DNA binding motif. The NH_2-termini of the two HTH motifs in the $TetR^D$ dimer face each other, whereas they are in opposite directions in other HTH motifs (Fig. 1B). The recognition helix α3 binds to the DNA major groove with inversed polarity, in agreement with a loss-of-contact analysis (*11*) and with TetR mutants exhibiting new operator recognition specificities (*12*). A comparable geometry was shown by nuclear magnetic resonance studies for the monomeric *lac* repressor headpiece in complex with half-operator DNA and verified on the basis of genetic data for the *lac* family (*13*). Because *lac* and

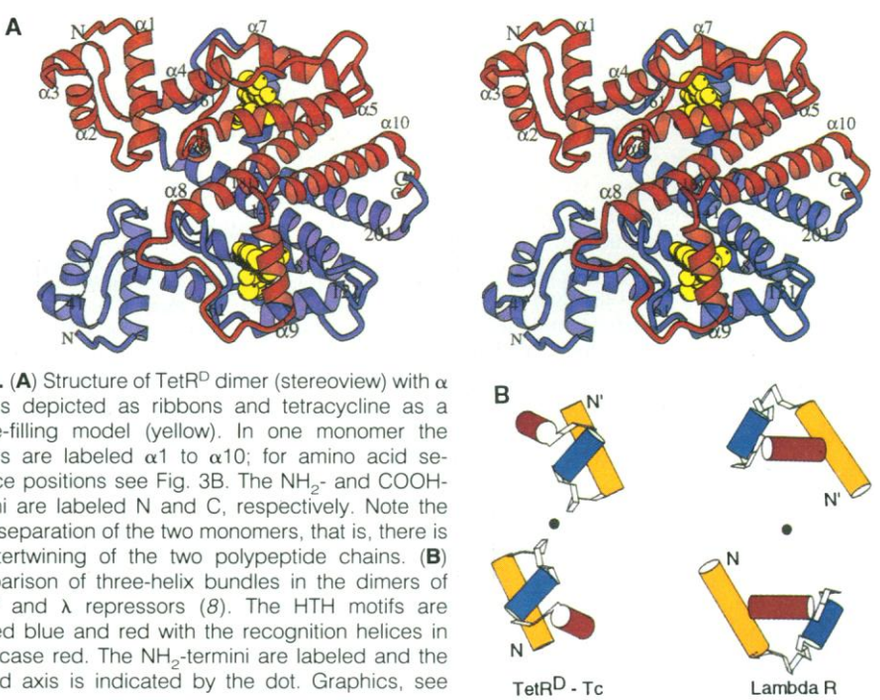

Fig. 1. (**A**) Structure of $TetR^D$ dimer (stereoview) with α helices depicted as ribbons and tetracycline as a space-filling model (yellow). In one monomer the helices are labeled α1 to α10; for amino acid sequence positions see Fig. 3B. The NH_2- and COOH-termini are labeled N and C, respectively. Note the clear separation of the two monomers, that is, there is no intertwining of the two polypeptide chains. (**B**) Comparison of three-helix bundles in the dimers of $TetR^D$ and λ repressors (*8*). The HTH motifs are colored blue and red with the recognition helices in each case red. The NH_2-termini are labeled and the twofold axis is indicated by the dot. Graphics, see (*28*).

W. Hinrichs, C. Kisker, M. Düvel, A. Müller, W. Saenger, Institut für Kristallographie, Freie Universität Berlin, 14195 Berlin, Germany.
K. Tovar and W. Hillen, Institut für Mikrobiologie und Biochemie der Friedrich-Alexander Universität, Erlangen-Nürnberg, 91058 Erlangen, Germany.
*To whom correspondence should be addressed.

Tet repressors require specific inducers to adopt the conformation that does not bind to DNA, there could be a distinct structure-function correlation.

Drug recognition in the $TetR^D$–[Mg-Tc]$^+$ structure (Fig. 2) is mediated by Mg^{2+} coordination and hydrogen bonding with side chains of amino acids conserved in all known TetR sequences (6). The Mg^{2+} is octahedrally coordinated by the chelating ketoenolate group O-11/O-12 of Tc, $His^{100}N\epsilon$, and by three water molecules in meridional arrangement. Two of the water ligands are hydrogen bonded to the carboxylate of Glu^{147}. Simultaneously $Gln^{116}N\epsilon H$ and $His^{64}N\epsilon H^+$ donate two three-center hydrogen bonds to the Tc amide oxygen in position 2 and to the negatively charged O-3. The enolate O-3 and the positively charged ammonium N-4 are bridged by hydrogen bonding to the amide side chain of Asn^{82}. The hydroxyl group O-121 of Tc forms an aromatic hydrogen bond (*14*) with the phenyl ring of Phe^{86}. This interaction seems to be of importance because amino acids in positions 85, 86, and 87 are identical in all known TetR sequences (6). The hydroxyl group in position 6 of Tc is in unfavorable van der Waals contact with the hydrophobic side chain of Val^{113}, explaining why elimination of O-6 in 5a,6-anhydrotetracycline enhances the affinity to $TetR^B$ (*15*). This scheme is augmented by hydrophobic interactions (Fig. 2).

Because the amino acids interacting with [Mg-Tc]$^+$ are conserved or type-conserved in all known TetR classes (6), they will provide a comparable recognition scheme. Modifications of functional groups in Tc involved in hydrogen bonding or Mg^{2+} coordination (ring A and positions 10, 11, 12, and 121) abolish antibiotic activity (*16*). In contrast, modifications of those groups that are only in hydrophobic contact with the protein are permissible. The known interactions between $TetR^D$ and [Mg-Tc]$^+$ may guide design of Tc analogs that still interact with the ribosome but do not change TetR conformation.

The $TetR^D$–[Mg-Tc]$^+$ complex is functionally unable to bind to operator DNA. The reason is the center-to-center separation between the recognition helices α3 and α3′ of 39 Å, which is ~5 Å too wide for interaction with adjacent major grooves of canonical B-form DNA (B-DNA). Computer-aided modeling (*17*) suggested that in the absence of [Mg-Tc]$^+$, the DNA binding domains can approach the assumed 34 Å spacing of α3 and α3′ for binding to straight B-DNA (*9*). The resulting model of the $TetR^D$–operator DNA complex shows protein-DNA contacts as identified by mutation and footprinting studies (*11, 18*). The modeling required mechanical tilting and rotation of the long helix α4 that acts as a lever with the short helix α6 as a seesaw (Fig. 3A). Both helices carry histidines at their COOH-termini (His^{64} and His^{100}) which bind to [Mg-Tc]$^+$. These His residues are strictly conserved in all known TetRs (6). The residue His^{100} is part of a loop (Arg^{104}, Pro^{105}) in the Tc binding pocket (α5, α6, α7, α8, α8′, and α9′) where the drug is strongly bound to the assumed rigid protein core (5). The end of the lever α4 is moved toward the protein core by [Mg-Tc]$^+$ binding to His^{64} so that the DNA binding domains, NH_2-terminal to α4, are moved in opposite directions and fixed in the observed position. A ligand-induced movement of the DNA binding domains is also known for *trp* repressor (*19*). In the inactive *trp* repressor, tryptophan is absent

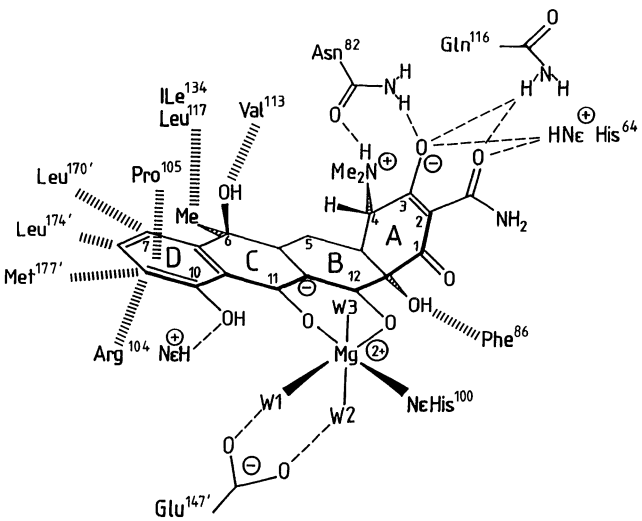

Fig. 2. Chemical structure of tetracycline and schematic description of the interactions between tetracycline and $TetR^D$. Dashed lines, hydrogen bonds; hatched lines, hydrophobic interactions. W1, W2, and W3 are water ligands in the octahedral coordination shell of Mg^{2+} and Me is methyl. Charges are marked (+) and (−).

Table 1. The $TetR^D$ was crystallized in complex with Tc (tetragonal space group $I4_122$ $a = b = 68.32$ Å, $c = 181.14$ Å) with one monomer per asymmetric unit. Diffraction data were collected with an Enraf-Nonius FAST area detector or a MAR Research Image Plate detector mounted on an FR571 rotating anode or an Image Plate detector (*22*) at the European Molecular Biology Laboratory (EMBL) outstation at DESY (Hamburg) on beamline X31. Data were processed with the MADNES system (*23*) for FAST data and MOSCO (*24*) for Image Plate data. Crystallographic computing was done with the CCP4 program package (*24*) with exceptions mentioned. We prepared the heavy-atom derivatives by soaking native crystals in the corresponding heavy-atom solution, and 7-iodo-6-deoxy-6-demethyltetracycline (7-iodo-Tc) was cocrystallized with $TetR^D$. Heavy-atom sites in the derivatives were located by difference Patterson techniques; minor sites were obtained from difference Fourier synthesis. An initial multiple isomorphous replacement (MIR) electron density map was calculated at 2.8 Å resolution (mean figure of merit 0.80 and 0.68 for centric and acentric reflections, respectively) and improved by solvent flattening (*25*). The polypeptide chain was traced unambiguously (*26*), excluding a weak density region from 155 to 165. Refinement by simulated annealing with X-PLOR (*27*) reduced the *R* factor from 37 to 28% for all data to 2.8 Å. The resolution was then extended to 2.5 Å which was followed by restrained positional and individual *B*-factor refinement. The NH_2-terminal and partial amino acid sequencing is in agreement with the final model, which comprises residues Ala^2 to Val^{208}, [Mg-Tc]$^+$, and 79 water molecules yielding an *R* factor of 19.5%. The φ,ψ angles lie in the allowed regions of the Ramachandran plot, some exceptions being the residues in the flexible loop 155 to 165, where the electron density is weakly defined and fragmented. The coordinates have been deposited with the Brookhaven Protein Data Bank. IP, Image Plate (HH, Hamburg; B, Berlin); $R_{sym} = \Sigma(|\langle I\rangle - I|)/\Sigma\langle I\rangle$, where I is the observed intensity and $\langle I\rangle$ is the averaged intensity obtained from multiple measurements of symmetry-related reflections. The mean isomorphous difference is $\Sigma\,||F_{PH}| - |F_P||/\Sigma|F_P|$, where $|F_P|$ and $|F_{PH}|$ are the protein and derivative structure amplitudes. The rms deviations from ideal bonds and angles were 0.017 Å and 3.30°, respectively.

	Detector	Wavelength (Å)	Resolution (Å)	Unique reflections	Completeness (%)	R_{sym}	Mean isomorphous difference
Native	IP, HH	0.9	10–2.5	8505	94.0	6.5	–
$CdCl_2$	IP, B	CuKα	10–2.8	5029	88.4	5.8	14.3
$K[Au(CN)_2]$	IP, HH	1.008	10–2.8	4726	83.1	6.2	25.1
$HgCl_2$	FAST, B	CuKα	10–3.0	3419	73.6	6.1	16.3
K_2PtBr_4	FAST, B	CuKα	10–3.4	2343	71.0	5.0	29.5
7-iodo-Tc	IP, HH	1.08	10–2.8	5546	99.3	5.8	28.9
7-iodo-Tc	FAST, B	CuKα	12–3.2	3228	85.0	4.0	23.4

and the HTH-containing domains are moved and tilted inward to shorten the 34 Å distance, thereby abolishing DNA binding.

A number of noninducible $TetR^B$ variants with single amino acid substitutions were characterized (*20*). These studies could not differentiate between loss of affinity for Tc and loss of the potential for conformational changes in TetR. The mutational data obtained with $TetR^B$ can be interpreted on the basis of the structure of $TetR^D$, because $TetR^B$ and $TetR^D$ share 63% sequence identity and their three-dimensional structures have the same peptide folding (*21*). It is of note that single amino acid substitution impairs $[Mg\text{-}Tc]^+$ binding or prevents the conformational change, although there are so many protein-drug interactions (Fig. 3B). This suggests that the specific drug recognition and positioning in the pocket is crucial for the function of TetR. If only those variants are considered in which induction by 5a,6-anhydrotetracycline is severely impaired, we find one subset of amino acid substitutions located in the Tc binding pocket. Other mutants are located on both sides of the short α6 which, according to our model, serves as a seesaw. Because these residues are not directly involved in Tc binding, we assume that they interfere with mediation of the conformational change of the DNA binding domains. These mutations clearly support the model suggested above for the structural change required for TetR release from operator DNA. The third group of important amino acids are adjacent to amino acids in the Tc binding pocket and close to the dimerization surface of the two monomers. They could interfere with TetR function by local structural changes. Furthermore, substitution of other amino acids that are located close to the twofold axis in the protein core suggests that the operator binding conformation of TetR depends also on dimer stability (*20*).

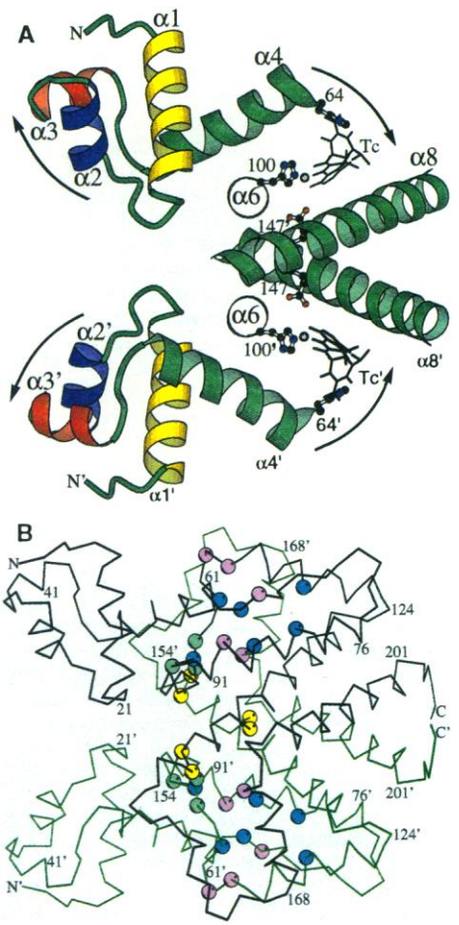

Fig. 3. (**A**) Schematic diagram (*28*) of the parts of $TetR^D$ that are essential for induction. The α6 acts as a seesaw and is tightly bound to the protein core through α8. The lever α4 moves the DNA binding domain, α1 to α3 (color code like Fig. 1B), triggered by binding of $[Mg\text{-}Tc]^+$ (Tc wire models, Mg^{2+} as single spheres) to amino acids His^{64}, His^{100}, and Glu^{147} (ball-and-stick). The arrows indicate local movement of α4 and of the DNA binding domains as suggested by model studies. (**B**) Cα trace (*28*) of the $TetR^D$ dimer with point mutations indicating three groups of noninducible variants. Residues in positions 64, 82, 86, 100, 105, and 116 (blue) interact with $[Mg\text{-}Tc]^+$; those in positions 93, 102, and 103 (green) are probably involved in signaling of conformational changes; those in positions 65, 89, 107, 109, and 178 (violet) are adjacent to amino acids interacting with $[Mg\text{-}Tc]^+$; and 144, 150, and 151 (yellow) are close to the twofold rotation axis and affect dimer stability of $TetR^D$.

REFERENCES AND NOTES

1. H. C. Neu, *Science* **257**, 1064 (1992).
2. S. B. Levy, in *Antimicrobial Drug Resistance*, L. E. Bryan, Ed. (Academic Press, New York, 1984), pp. 191–240; *Am. Soc. Microbiol. News* **54**, 418 (1988).
3. M. Kaneko, A. Yamaguchi, T. Sawai, *FEBS Lett.* **193**, 194 (1985); A. Yamaguchi, N. Ono, T. Akasaka, T. Noumi, T. Sawai, *J. Biol. Chem.* **265**, 15525 (1990).
4. W. Hillen, C. Gatz, L. Altschmied, K. Schollmeier, I. Meier, *J. Mol. Biol.* **169**, 707 (1983).
5. M. Takahashi, L. Altschmied, W. Hillen, *ibid.* **187**, 341 (1986).
6. There are at least six determinants of *tetR*, classes A to E and G, that share a common genetic organization. Tet repressors B and D as well as A, C, and G compose two subgroups which have at least 60% sequence identity within the subgroups. B. Mendez, C. Tachibana, S. B. Levy, *Plasmid* **3**, 99 (1980); B. Unger, G. Klock, W. Hillen, *Nucleic Acids Res.* **12**, 7693 (1984); K. Tovar, A. Ernst, W. Hillen, *Mol. Gen. Genet.* **215**, 76 (1988); J. Zhao and T. Aoki, *Microbiol. Immunol.* **36**, 1051 (1992).
7. R. Baumeister, G. Müller, B. Hecht, W. Hillen, *Proteins Struct. Funct. Genet.* **14**, 168 (1992); C. Berens, L. Altschmied, W. Hillen, *J. Biol. Chem.* **267**, 1945 (1992).
8. D. Kostrewa *et al.*, *J. Mol. Biol.* **226**, 209 (1992); S. C. Schultz, G. C. Shields, T. A. Steitz, *ibid.* **213**, 159 (1990); R. G. Brennan, S. L. Roderick, Y. Takeda, B. W. Matthews, *Proc. Natl. Acad. Sci. U.S.A.* **87**, 8165 (1990); S. R. Jordan and C. O. Pabo, *Science* **242**, 893 (1988); A. K. Aggarwal, D. W. Rodgers, M. Drottar, M. Ptashne, S. C. Harrison, *ibid.*, p. 899; Z. Otwinowski *et al.*, *Nature* **335**, 321 (1988).
9. S. C. Harrison, *Nature* **353**, 715 (1991).
10. K. Postle, T. T. Nguyen, K. P. Bertrand, *Nucleic Acids Res.* **12**, 4849 (1984); P. J. Isackson and K. P. Bertrand, *Proc. Natl. Acad. Sci. U.S.A.* **82**, 6226 (1985).
11. A. Wissmann *et al.*, *EMBO J.* **10**, 4145 (1991).
12. R. Baumeister, V. Helbl, W. Hillen, *J. Mol. Biol.* **226**, 1257 (1992); C. Sizemore, A. Wissmann, U. Gülland, W. Hillen, *Nucleic Acids Res.* **18**, 2875 (1990).
13. R. M. J. N. Lamerichs, R. Boelens, G. A. van der Marel, J. H. van Boom, R. Kaptein, *Eur. J. Biochem.* **194**, 629 (1990); N. Lehming, J. Sartorius, S. Oehler, B. von Wilcken-Bergmann, B. Müller-Hill, *Proc. Natl. Acad. Sci. U.S.A.* **85**, 7947 (1988).
14. S. Suzuki *et al.*, *Science* **257**, 942 (1992).
15. J. Degenkolb, M. Takahashi, G. A. Ellestad, W. Hillen, *Antimicrob. Agents Chemother.* **35**, 1591 (1991).
16. J. J. Hlavka and J. H. Boothe, Eds., *Handbook of Experimental Pharmacology* (Springer-Verlag, Berlin, 1985), vol. 78, pp. 332–334.
17. Bending and curvature of operator DNA as a result of TetR binding has been reported [K. Tovar and W. Hillen, *Nucleic Acids Res.* **17**, 6515 (1989)], but is most likely too small to compensate for spacing and rotation of the DNA binding domains.
18. K. P. Bertrand, K. Postle, L. V. Wray, W. S. Reznikoff, *Gene* **23**, 149 (1983); W. Hillen, K. Schollmeier, C. Gatz, *J. Mol. Biol.* **172**, 185 (1984); C. Heuer and W. Hillen, *ibid.* **202**, 407 (1988).
19. R.-G. Zhang *et al.*, *Nature* **327**, 591 (1987).
20. L. D. Smith and K. P. Bertrand, *J. Mol. Biol.* **203**, 949 (1988); B. Hecht, G. Müller, W. Hillen, *J. Bacteriol.* **175**, 1206 (1993).
21. The refined coordinates of the $TetR^D$–$[Mg\text{-}Tc]^+$ complex were used for structure elucidation of TetR, class B. The $TetR^B$–$[Ba\text{-}5a,6\text{-anhydrotetracycline}]^+$ complex was crystallized according to H. E. Parge *et al.* [*J. Mol. Biol.* **180**, 1189 (1984)]. Diffraction data to 3.2 Å resolution (space group $P4_12_12$, $a = b = 73.76$ Å, $c = 93.99$ Å) were used for molecular replacement [X-PLOR, A. T. Brünger, *Acta Crystallogr. A* **46**, 46 (1990)]. Structure refinement confirmed identical peptide folding of $TetR^B$.
22. Z. Dauter, H. Terry, H. Witzel, K. S. Wilson, *Acta Crystallogr. B* **46**, 833 (1990).
23. A. Messerschmidt and J. W. Pflugrath, *J. Appl. Crystallogr.* **20**, 306 (1987).
24. CCP4, Science and Engineering Research Council (SERC), Collaborative Computing Project no. 4, SERC Daresbury Laboratory, Warrington, United Kingdom (1979).
25. B. C. Wang, *Methods Enzymol.* **115**, 90 (1985).
26. T. A. Jones, *J. Appl. Crystallogr.* **11**, 268 (1978).
27. A. T. Brünger, J. Kuriyan, M. Karplus, *Science* **235**, 458 (1987).
28. P. J. Kraulis, *J. Appl. Crystallogr.* **24**, 946 (1991); A. M. Lesk and K. D. Hardman, *Science* **216**, 539 (1982).

29. Protein sequencing by W. Schröder (Berlin), initial help with synchrotron data processing by Z. Dauter (Hamburg), and continuous support for data collection at the EMBL outstation at DESY are gratefully acknowledged. Supported by Fonds der Chemischen Industrie and by the Deutsche Forschungsgemeinschaft through regular grants and Schwerpunktprogramm "Biophysik der Zelle," Sonderforschungsbereich 344, and Leibniz-Programm. K.H.T. and W.H. were supported by the Wilhelm Sander Stiftung. We thank G. A. Ellestad and P. E. Sum (American Cyanamid Company, Lederle Laboratory, United States) for providing 7-iodo-6-deoxy-6-demethyltetracycline.

16 November 1993; accepted 28 February 1994